PHYSICAL REVIEW A **79**, 061403(R) (2009)

Production of heteronuclear molecules in an electronically excited state by photoassociation in a mixture of ultracold Yb and Rb

N. Nemitz, F. Baumer, F. Münchow, S. Tassy, and A. Görlitz
Institut für Experimentalphysik, Heinrich-Heine-Universität Düsseldorf, Universitätsstraße 1, 40225 Düsseldorf, Germany
(Received 5 July 2008; published 4 June 2009)

We have produced ultracold heteronuclear YbRb* molecules in a combined magneto-optical trap by photoassociation. The formation of electronically excited molecules close to the dissociation limit was observed by the trap loss spectroscopy in mixtures of ^{87}Rb with ^{174}Yb and ^{176}Yb. The molecules could be prepared in well-defined rovibrational levels, allowing for an experimental determination of the long-range potential in the electronically excited state.

DOI: 10.1103/PhysRevA.79.061403 PACS number(s): 37.10.Mn, 33.15.−e, 33.80.−b, 34.20.Cf

Ultracold polar molecules offer fascinating prospects for the realization of new forms of quantum matter [1] with possible applications to quantum information [2] and to precision measurements [3,4]. While dense atomic clouds are routinely laser cooled to μK temperatures, the complex internal structure of molecules has so far prevented this direct method. Among various approaches currently under investigation [5], the production of translationally cold molecules from mixed-species ensembles of ultracold atoms is one of the most promising.

The possible routes for the conversion from atoms to molecules involve either the use of magnetically tunable Feshbach resonances [6] or the light-assisted photoassociation (PA) [7]. While Feshbach resonances are a highly efficient method to produce vibrationally excited molecules in the electronic ground state, they are not sufficient to access low-lying rovibrational levels and experimentally accessible Feshbach resonances do not necessarily exist for all atomic mixtures [6]. In contrast, photoassociation is generally applicable to all combinations of atomic species, albeit so far its experimental demonstration has been restricted to mixtures of alkalis [8–12]. Recently, optical trapping [13] and the observation of molecules in the rovibrational ground state [14] have been reported in such bialkali systems. A major breakthrough on the way toward quantum degenerate gases of deeply bound molecules is the combination of Feshbach molecule production with two-photon state transfer [15,16], which led very recently to the coherent production of homonuclear and heteronuclear molecular gases in the rovibrational ground state [17,18].

In this Rapid Communication, we report on the controlled production of ultracold heteronuclear molecules in a mixture of the alkali rubidium (Rb) and the rare-earth ytterbium (Yb). The molecules are created in an electronically excited state by a single-photon photoassociation. While the ultimate goal is the production and detection of ground-state molecules, this is another decisive step toward a different class of dipolar molecules. The main difference between bialkalis and YbRb is that the electronic ground state of bialkalis is always a $^1\Sigma_0$, while in YbRb it is a $^2\Sigma_{1/2}$ state. This implies that ground-state YbRb molecules possess a significant magnetic-dipole moment, in addition to their electric-dipole moment, and can thus be trapped and manipulated using magnetic fields. An intriguing prospect for such ultracold molecules with an unpaired electron is the realization of lattice-spin models [19].

Our experiments were performed using a continuously loaded double-species magneto-optical trap (MOT). Typically, 10^9 ^{87}Rb atoms are trapped in a forced dark-spot MOT [20] which is loaded from a Zeeman slower. The resulting atom cloud has a diameter of 2 mm [full width at half maximum (FWHM)] and a temperature of $T_{\mathrm{Rb}}=340$ μK, where $>95\%$ of the atoms are in the dark $F=1$ state. The Yb MOT operates on the $6\,^1S_0 \rightarrow 6\,^3P_1$ intercombination transition at 556 nm and is loaded from a Zeeman slower operating on the fast $6\,^1S_0 \rightarrow 6\,^1P_1$ transition at 399 nm. It holds 4×10^7 atoms in a 0.5 mm cloud at $T_{\mathrm{Yb}}=510$ μK when there is no Rb present. With the Rb MOT on, the number of Yb atoms drops to 2×10^6 atoms due to Yb*-Rb collisions and the exponential loading time is typically 0.2 s.

Here, we concentrate on the photoassociation close to the $5\,^2S_{1/2} \rightarrow 5\,^2P_{1/2}$ transition of Rb at 795 nm (D1 line) which is investigated by superimposing a PA laser onto the two overlapped MOTs. The PA laser beam with a power of up to 440 mW (resulting in a peak intensity of $I_{\mathrm{max}}=400$ W/cm^2 at the MOT position) is provided by a Ti:sapphire laser with a scanning range of 4 GHz. Molecule formation is detected by observing an additional loss of Yb from the MOT when the PA laser is resonant with a transition from an unbound atom pair to an YbRb*-excited state. The loss occurs since most of the excited molecules decay into hot atoms or ground-state molecules which are both not trapped in the MOTs [7]. Due to the strong imbalance in atom numbers, this leaves the Rb MOT virtually unchanged, while the loss of Yb atoms can be significant.

In the following, all wave numbers are given as the detuning Δ_{PA} of the PA laser from the $F=1 \rightarrow F'=2$ transition of the D_1 line of Rb as depicted in Fig. 1. Thus, Δ_{PA} is a direct measure for the binding energy of the formed molecules. In our measurement sequence, the PA laser is swept over its full scanning range with a frequency of 10 mHz, while the power of the Yb fluorescence P_{fluor} is recorded as a measure for the number of trapped Yb atoms. Typically, four sweeps are averaged to obtain photoassociation spectra of individual lines as depicted in Figs. 2(b)–2(d). Since there is no effect of the PA laser on a pure Yb cloud, any decrease in fluorescence can be attributed to Yb-Rb photoassociation [21].

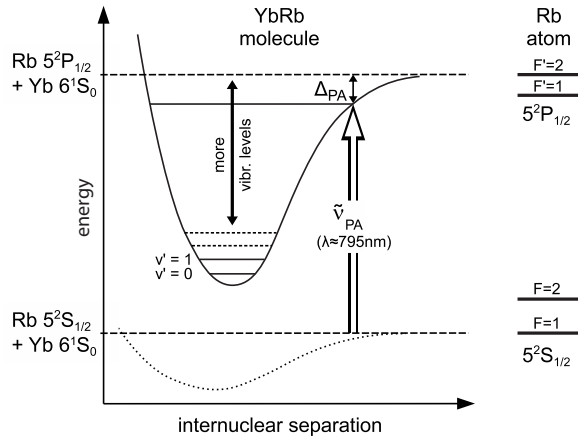

FIG. 1. Relevant level structure (not to scale) in the YbRb molecule and the Rb atom close to the D_1 line of Rb at 795 nm. The detuning from resonance in wave numbers is defined as $\Delta_{PA}=\tilde{\nu}_{PA}-\tilde{\nu}_{res}$ with $\tilde{\nu}_{res}=12\,578.862$ cm^{-1}.

It is not immediately clear whether the observed photoassociation loss stems from the formation of singly excited YbRb* or doubly excited Yb*Rb* since ground- and excited-state atoms are present in the Yb MOT. To rule out the formation of Yb*Rb*, we have performed tests in which the atoms were only exposed to the PA light within a periodically recurring dark phase of 50 μs in which the Yb MOT light is switched off. During this dark phase, all Yb atoms return to the ground state. While the efficiency of the MOT is reduced, photoassociation is still clearly observed under this condition, demonstrating that indeed singly excited YbRb* molecules are formed.

Figure 2(a) shows a partial spectrum for ^{176}Yb ^{87}Rb*. The absolute error of the wave-number determination is $\pm 5\times10^{-3}$ cm^{-1}, while the relative position of the components of a vibrational line [Figs. 2(b)–2(d)] could be determined with a resolution of 2×10^{-4} cm^{-1}, which is close to the Doppler-broadened linewidth for a photoassociation line at the effective temperature of 450 μK. Only lines for $\Delta_{PA}<-0.38$ cm^{-1} could be observed since the PA laser significantly interferes with the Rb MOT performance if its frequency is too close to the atomic resonance. For $\Delta_{PA}<-8$ cm^{-1}, several additional lines were found by scanning over a small range in the vicinity of line positions which were extrapolated using Leroy-Bernstein methods [22,23]. For the strongest line at $\Delta_{PA}\approx-2.7$ cm^{-1}, we determine a loss rate per Yb atom of $\Gamma_{PA}\approx1.4$ s^{-1} corresponding to a total production rate of excited-state YbRb* molecules of $\approx1.9\times10^6$ s^{-1}. This is similar to the results of a comparable experiment with rubidium and cesium [24], where a trap loss rate of 0.5 s^{-1} per cesium atom was measured and is also in agreement with theoretical predictions based on [7].

The majority of observed lines belongs to a vibrational series converging on the excited 5 $^2P_{1/2}$ state of Rb. Each vibrational level shows two separate rotational progressions corresponding to the $F'=1$ and $F'=2$ states of the Rb atom where the observed hyperfine splitting is close to the atomic value of 0.0273 cm^{-1}. Table I lists the wave numbers and relative strengths for the stronger $F'=2$ components of all investigated lines including some lines in ^{174}Yb ^{87}Rb* that were investigated to check our model of the molecular structure for consistency. Because of the shorter range of the excited-state potential in heteronuclear as compared to homonuclear molecules, oscillations in the Franck-Condon factor happen on an energy scale comparable to the vibrational spacing [25], causing the observed strong fluctuations of the line strength. We have been unable to find the $\Delta v'=-20$ and $\Delta v'=-22$ lines in ^{176}Yb ^{87}Rb*, probably due to a

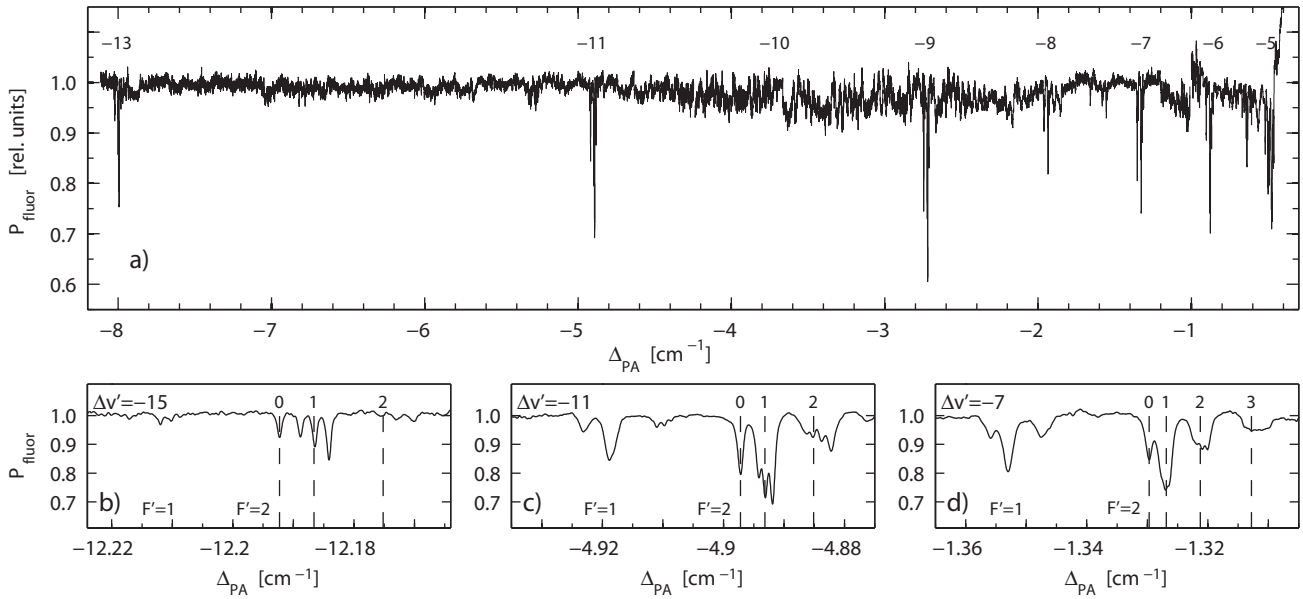

FIG. 2. (a) Photoassociation spectrum in a mixture of ^{176}Yb and ^{87}Rb. Relative vibrational quantum numbers $\Delta v'=v'-v'_{max}$ of vibrational levels in the excited state are indicated for observed lines. [(b)–(d)] Resolved rotational structure for selected levels. More tightly bound vibrational levels exhibit a larger rotational splitting and, in addition, a splitting of the rotational components. For all lines, two hyperfine components corresponding to the 5 $^2P_{1/2}$, $F'=1$, and $F'=2$ levels of ^{87}Rb are observed.

TABLE I. Observed lines in ^{176}Yb ^{87}Rb* and ^{174}Yb ^{87}Rb*. $\Delta_{\mathrm{PA},R'=0}$ refers to the $R'=0$ component of a vibrational line, $\Delta v' = v' - v'_{\max}$ is the relative vibrational quantum number, and $\Delta_{R'=1}$ the spacing between adjacent components of the $R'=1$ component. The effective internuclear distance r'_{eff} is calculated from the rotational constant B_{rot}.

$\Delta_{\mathrm{PA},R'=0}$ (cm^{-1})	$\Delta v'$	Relative strength[a]	$\Delta_{R'=1}$ (10^{-3} cm^{-1})	$B_{\mathrm{rot}}/(hc)$ (10^{-3} cm^{-1})	r'_{eff} (a_0)
		^{176}Yb ^{87}Rb , $F'=2$ state			
−0.494	−5	0.03	n.r.[b]	0.85	34.9
−0.881	−6	0.10	2.0	1.45	26.7
−1.330	−7	0.15	0.7	1.34	27.8
−1.938	−8	0.09	0.7	1.48	26.4
−2.723	−9	0.27	0.8	1.65	25.0
−3.707	−10	0.02	0.8	1.66	25.0
−4.897	−11	0.20	1.1	2.00	22.8
−6.333	−12	0.02	1.5	2.00	22.8
−8.001	−13	0.16	1.5	2.45	20.6
−9.950	−14	0.02	1.7	2.47	20.5
−12.192	−15	0.08	2.4	2.90	18.9
−14.808	−16	0.06	2.5	2.98	18.6
−17.687	−17	0.05	2.6	3.14	18.2
−20.921	−18	0.10	2.9	3.30	17.7
−24.553	−19	0.01	2.5	3.35	17.6
−33.055	−21	0.02	2.3	3.60	17.0
		^{174}Yb ^{87}Rb, $F'=2$ state			
−0.425	−4	0.09	n.r.[b]	1.02	31.9
−0.728	−5	0.10	0.27	1.09	30.9
−1.149	−6	0.18	0.50	1.40	27.2
−2.437	−8	0.17	0.7	1.67	24.9
−4.459	−10	0.15	1.1	1.95	23.1
−7.384	−12	0.11	1.7	2.33	21.1
		Accuracy			
±0.005		±0.02	±0.2	±0.15	

[a]Relative loss of fluorescence for $R'=0$ component.
[b]Not resolved.

Franck-Condon overlap that is too small to lead to a detectable trap loss.

All observed lines show resolved rotational components according to $E_{\mathrm{rot}}=B_{\mathrm{rot}}R'(R'+1)$ where B_{rot} is the rotational constant and R' is the quantum number for the rotation of the nuclei in the excited state as shown in Figs. 2(b)–2(d). Due to the temperature of just several 100 μK, only $R'=0,1,2$ components were observed for most lines since the ground-state centrifugal barrier for the $R=3$ component at 114 a_0 has a height of 916 μK. For lines with small Δ_{PA}, more rotational components were detected [see Fig. 2(d)] since under this condition the Rb MOT is heated up by the PA laser. In the fixed-rotor approximation, the rotational constant is $B_{\mathrm{rot}}=\hbar^2/(2\mu r^2)$, where μ is the reduced mass and r is the distance of the nuclei. For the low rotational quantum numbers in our experiment, centrifugal stretching effects can be neglected and an effective fixed-rotor radius $r'_{\mathrm{eff}}=\hbar/\sqrt{2\mu B_{\mathrm{rot}}}$ may be defined for the excited YbRb* molecules, which is also listed in Table I.

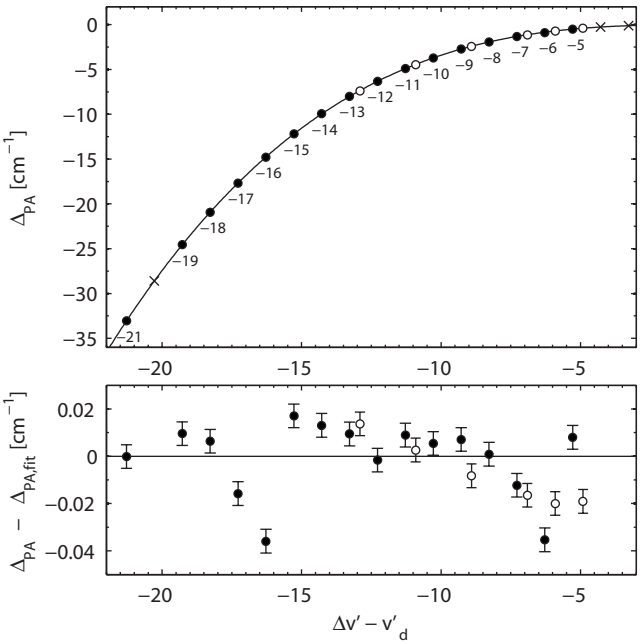

FIG. 3. (Top) Binding energy Δ_{PA} of vibrational lines ($R'=0$ component). The solid line is a fit to all ^{176}Yb ^{87}Rb* lines (●) according to the model of Ref. [23]. For the observed ^{176}Yb ^{87}Rb* lines, the relative vibrational quantum numbers $\Delta v'$ are indicated, while predicted but unobserved levels are marked by "x." The data points for ^{174}Yb ^{87}Rb* (○) are corrected for the mass difference. (Bottom) Difference between observed values and fit.

The finest observed structure is a splitting of the rotational components. The observed pattern agrees with a Hund's case (e) angular-momentum coupling, where the total nuclear and electronic angular momentum F' is that of the excited Rb atom ($F'=1$ or $F'=2$) with no contribution from Yb. The angular momentum F' then couples to the nuclear rotation R'. As Figs. 2(b) and 2(c) show, the number of observed components is compatible with the expectations for this case, while in Fig. 2(d) the individual components cannot be resolved due to the smaller splitting of the lines close to the dissociation limit. Taking into account the whole spectroscopic structure, the wave number of an individual line component is given by the experimentally determined constants in Table I as

$$\tilde{\nu}_{\mathrm{PA}} = \tilde{\nu}_{\mathrm{res}} + \Delta_{\mathrm{PA},R'=0} + \frac{B_{\mathrm{rot}}}{hc}R'(R'+1) + m'_{R'}\Delta_{R'}, \qquad (1)$$

where $m'_{R'}$ runs from $-R'$ to R' (or $-F'$ to F' for $R'>F'$).

In the near-dissociation limit, the vibrational energies are predominantly determined by the long-range dispersion coefficients. An improved Leroy-Bernstein method as described in Ref. [23] was used to assign vibrational quantum numbers and extract values for the dispersion coefficient C'_6. Since the total number of vibrational levels in the potential

well is unknown, Table I lists quantum numbers $\Delta v' = v' - v'_{max}$ relative to the last vibrational level. As Fig. 3 illustrates, the observed line positions are reproduced by a fit to the theoretical model of Ref. [23]. The fit yields $v'_d(^{176}Yb\ ^{87}Rb^*) = 0.278$ and $v'_d(^{174}Yb\ ^{87}Rb^*) = 0.906$ for the noninteger values of the relative vibrational quantum numbers at the dissociation limit and a dispersion coefficient $C'_6 = 5684 \pm 98$ a.u., which is similar to values predicted for other heteronuclear atom pairs [26].

The validity of our analysis of the YbRb* molecule can be tested by comparing the long-range potential $V'(r) = -C'_6/r^6$ (derived from the vibrational structure via the Leroy-Bernstein fit) and the effective internuclear distances r'_{eff} (obtained from the rotational structure). For a given vibrational wave function $\psi_{v'}(r)$, r'_{eff} can be approximated by $r'_{eff} = \sqrt{\int_{-\infty}^{\infty} \psi_{v'}(r)^2 r^2 dr}$. While r'_{eff} is always smaller than the classical outer turning point r'_{max} given by $\Delta_{PA} = V'(r'_{max})/(hc)$, the vibrational wave function is concentrated near r'_{max} for levels close to the dissociation limit. Therefore, it is expected that r'_{eff} is close to r'_{max}—but somewhat smaller—in qualitative agreement with our experimental finding (Fig. 4), which yields $r'_{eff} \approx 0.9 r'_{max}$ over the experimental range.

In conclusion, we have produced ultracold electronically excited YbRb* molecules in well-defined rovibrational levels by photoassociation. By precise determination of the position of the rovibrational levels close to the dissociation threshold, we were able to model the long-range part of the molecular potential. These results are invaluable steps toward the production of ultracold YbRb ground-state molecules. The route toward this goal will most likely involve two-color photoassociation to high-lying vibrational levels in the electronic ground state and subsequent transfer to low-lying vibrational levels as has recently been demonstrated [15–18]. We anticipate that the simpler structure of YbRb compared to the bialkalis will allow for a straightforward determination of the best path to the absolute ground state of the molecule. The next experimental step will combine the photoassociative production of ultracold molecules with conservative trapping of the Yb-Rb mixture which we have recently demonstrated [27].

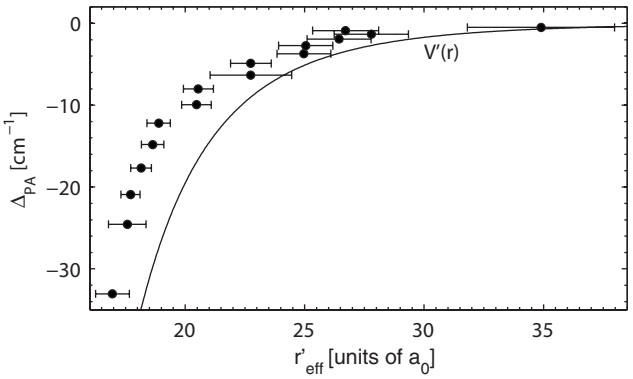

FIG. 4. Comparison of the Le-Roy Bernstein potential $V'(r)$ and r'_{eff} (●) for $^{176}Yb\ ^{87}Rb$. The observed difference between r'_{eff} and the potential curve is in qualitative agreement with theoretical considerations (see text).

We acknowledge stimulating discussions with T. Fleig. The project is supported by the DFG under Grant No. SPP 1116. F.B. was supported by the Stiftung der Deutschen Wirtschaft.

[1] M. Baranov *et al.*, Phys. Scr. **T102**, 74 (2002).
[2] D. DeMille, Phys. Rev. Lett. **88**, 067901 (2002).
[3] D. DeMille, S. B. Cahn, D. Murphree, D. A. Rahmlow, and M. G. Kozlov, Phys. Rev. Lett. **100**, 023003 (2008).
[4] E. R. Hudson, H. J. Lewandowski, B. C. Sawyer, and J. Ye, Phys. Rev. Lett. **96**, 143004 (2006).
[5] J. Doyle *et al.*, Eur. Phys. J. D **31**, 149 (2004).
[6] T. Kohler, K. Goral, and P. S. Julienne, Rev. Mod. Phys. **78**, 1311 (2006).
[7] K. M. Jones *et al.*, Rev. Mod. Phys. **78**, 483 (2006).
[8] D. Wang *et al.*, Phys. Rev. Lett. **93**, 243005 (2004).
[9] M. W. Mancini, G. D. Telles, A. R. L. Caires, V. S. Bagnato, and L. G. Marcassa, Phys. Rev. Lett. **92**, 133203 (2004).
[10] J. M. Sage, S. Sainis, T. Bergeman, and D. DeMille, Phys. Rev. Lett. **94**, 203001 (2005).
[11] S. D. Kraft *et al.*, J. Phys. B **39**, S993 (2006).
[12] U. Schloder, C. Silber, T. Deuschle, and C. Zimmermann, Phys. Rev. A **66**, 061403(R) (2002).
[13] E. R. Hudson, N. B. Gilfoy, S. Kotochigova, J. M. Sage, and D. DeMille, Phys. Rev. Lett. **100**, 203201 (2008).
[14] J. Deiglmayr *et al.*, Phys. Rev. Lett. **101**, 133004 (2008).
[15] S. Ospelkaus *et al.*, Nat. Phys. **4**, 622 (2008).
[16] J. G. Danzl *et al.*, Science **321**, 1062 (2008).
[17] F. Lang, K. Winkler, C. Strauss, R. Grimm, and J. Hecker Denschlag, Phys. Rev. Lett. **101**, 133005 (2008).
[18] K. K. Ni *et al.*, Science **322**, 231 (2008).
[19] A. Micheli, G. K. Brennen, and P. Zoller, Nat. Phys. **2**, 341 (2006).
[20] M. H. Anderson, W. Petrich, J. R. Ensher, and E. A. Cornell, Phys. Rev. A **50**, R3597 (1994).
[21] Rb-Rb photoassociation only has a small effect on the Yb signal, leading to a slight increase in the Yb fluorescence due to the reduced Rb-induced loss.
[22] R. J. LeRoy and R. B. Bernstein, J. Chem. Phys. **52**, 3869 (1970).
[23] D. Comparat, J. Chem. Phys. **120**, 1318 (2004).
[24] A. J. Kerman, J. M. Sage, S. Sainis, T. Bergeman, and D. DeMille, Phys. Rev. Lett. **92**, 033004 (2004).
[25] S. Azizi, M. Aymar, and O. Dulieu, Eur. Phys. J. D **31**, 195 (2004).
[26] M. Marinescu and H. R. Sadeghpour, Phys. Rev. A **59**, 390 (1999).
[27] S. Tassy *et al.*, e-print arXiv:0709.0827.